Structural Engineering and Mechanics, Vol. 5, No. 6 (1997) 755-765
DOI: http://dx.doi.org/10.12989/sem.1997.5.6.755

The effect of constitutive spins on finite inelastic strain simulations

Han Wook Cho†

Institute of Technology, Eng. & Construction Group, Samsung Corporation, San 25, Gongse-ri, Giheung-eup, Yongin-city, Kyunggi-do 449-900, Korea

Yannis F. Dafalias‡

Division of Mechanics, National Technical University of Athens, 5 Heroes of Polytechnion Avenue, Zorgraphou 15773, Greece and Department of Civil & Environmental Engineering, University of California, Davis, CA 95616, U.S.A.

Abstract. Within the framework of anisotropic combined viscoplastic hardening formulation, accounting macroscopically for residual stress as well as texture development at finite deformations of metals, simple shear analyses for the simulation of fixed-end torsion experiments for *α-Fe*, *Al* and *Cu* at different strain rates are reviewed with an emphasis on the role of constitutive spins. Complicated responses of the axial stresses with monotonically increasing shear deformations can be successfully described by the capacity of orthotropic hardening part, featuring tensile axial stresses either smooth or oscillatory. Temperature effect on the responses of axial stresses for *Cu* is investigated in relation to the distortion and orientation of yield surface. The flexibility of this combined hardening model in the simulation of finite inelastic strains is discussed with reference to the variations of constitutive spins depending upon strain rates and temperatures.

Key words: anisotropic viscoplastic hardening; constitutive; plastic spin; kinematic; orthotropic; distortional; orientational; yield surface.

1. Introduction

Initial random orientation of grains in a metal tends to acquire directional properties with plastic deformations. This phenomenon is most often explained in a macroscopic way by locked-in residual stress (back stress) of kinematic hardening and/or texture development within anisotropic hardening formulation. While a kinematic hardening model can describe the back stress developed within grain boundaries and the grains themselves due to the differential orientations of grains, it cannot account for texture developments at large plastic deformations, for which Hill (1950) proposed orthotropic yield criterion with no back stress terms as a simple case of anisotropy. In addition, he just assumed that the orthotropic axes of anisotropic hardening material be considered aligned with the principal stretch directions without mentioning how initial isotropy of a material evolves towards orthotropy with plastic deformations, which has continuous-

† General Manager, Ph.D.
‡ Professor

ly been the topic of Dafalias and Cho (1989), Dafalias (1993) and Cho and Dafalias (1996). In order to describe together two different phenomena of residual stress and orthotropy at finite inelastic deformations, Cho and Dafalias (1996) proposed a combined hardening anisotropic viscoplastic model with an introduction of multiple constitutive spin (total spin minus plastic spin) concept, employing separate evolutions for different physical variables. By solving analytical equations for simple shear case with an assumption of rigid plastic material, they presented the simulations in a good agreement with the fixed-end torsion experiments for *α-Fe, Al* and *Cu* (Montheillet, *et al.* 1984) at different strain rates, and discussed the variations of the axial stresses and their associated variations of yield surface for *Al* depending on temperature. Especially, oscillatory complex axial stresses with monotonically increasing shear strains were successfully explained at different strain rates in terms of the distortional and orientational hardenings of dynamic yield surface as well as classical isotropic/kinematic hardenings.

In this paper, following the general formulation of Cho and Dafalias (1996), the combined hardening viscoplastic model and simple shear analysis will be first summarized in the subsequent sections, and then the simulations for the aforementioned experiments will be in more detail investigated, focusing on the effect of constitutive spins via plastic spin terms on the responses of *α-Fe, Al* and *Cu* at three different strain rates. And the variations of axial stresses for *Cu* with shear deformations at various temperatures will be examined with reference to their associated yield surfaces. Finally, the variational trend of the plastic spins with temperature is discussed from the simulations of *Cu* as well as those of *Al* from the above reference.

Tensors will be denoted by boldface characters in direct notation. With the summation convention over repeated indices, the following symbolic operations are defined: $\boldsymbol{a}\boldsymbol{\sigma}=a_{ij}\sigma_{jk}$, $\boldsymbol{a}:\boldsymbol{\sigma}=a_{ij}\sigma_{ij}$, $\boldsymbol{a}\otimes\boldsymbol{\sigma}=a_{ij}\sigma_{kl}$ with proper extension to the tensors of different order. The prefix tr indicates the trace, and a superposed dot denotes the material time derivative or rate.

2. Combined hardening viscoplastic model

General kinematics and kinetics in large inelastic macroscopic formulation with the plastic spin concept were in a systematic way reviewed in Dafalias (1985, 1990). Bypassing the details thereof, Eulerian kinematics in small elastic and finite plastic deformations can be described as follows:

$$\boldsymbol{D}=\boldsymbol{D}^e+\boldsymbol{D}^p \tag{1}$$

$$\boldsymbol{W}=\boldsymbol{\omega}+\boldsymbol{W}^p=\boldsymbol{\omega}_c+\boldsymbol{W}_c^p \tag{2}$$

where $\boldsymbol{D}$, $\boldsymbol{D}^e$ and $\boldsymbol{D}^p$ denote the total, elastic and plastic rate of deformations, respectively, and $\boldsymbol{W}$, $\boldsymbol{\omega}$ and $\boldsymbol{W}^p$ the total, substructural and plastic rate of rotations or spins, respectively. The $\boldsymbol{\omega}_c$ denotes the constitutive spin for the rate equation of evolution for each internal variable, implying multiple spins for many variables. The $\boldsymbol{W}_c^p$ is the plastic spin associated with $\boldsymbol{\omega}_c$. The material state will be defined at the current configuration in terms of the Cauchy stress $\boldsymbol{\sigma}$ and a representative collection $\boldsymbol{a}$ of structure variables. It is assumed that the $\boldsymbol{a}$ provide anisotropic property via its tensorial character. The corotational rate of the $\boldsymbol{a}$, if it is a second order tensor, with respect to the constitutive spin $\boldsymbol{\omega}_c$ will be defined by

$$\overset{c}{\boldsymbol{a}}=\dot{\boldsymbol{a}}-\boldsymbol{\omega}_c\,\boldsymbol{a}+\boldsymbol{a}\boldsymbol{\omega}_c. \tag{3}$$

As mentioned in the previous section, a combined hardening anisotropic model (Cho and Dafalias 1996) was proposed to take into consideration isotropic/kinematic hardenings as well as orthotropic hardening evolution with the axes of orthotropy along the unit vectors $\boldsymbol{n}_i$. Denoting by superposed $\hat{}$ the tensor components in reference to the $\boldsymbol{n}_i$-axes, and by σ, $\boldsymbol{s}$ and α, the Cauchy stress, deviatoric Cauchy stress and deviatoric back stress tensors, respectively, and defining $\sigma^*=\sigma-\alpha$ and $\boldsymbol{s}^*=\boldsymbol{s}-\alpha$, a dynamic yield surface is given by

$$\begin{aligned}J\equiv&\{A(\hat{\sigma}_{11}^*-\hat{\sigma}_{22}^*)^2+B(\hat{\sigma}_{22}^*-\hat{\sigma}_{33}^*)^2+C(\hat{\sigma}_{33}^*-\hat{\sigma}_{11}^*)^2+2D\hat{\sigma}_{23}^{*2}+2E\hat{\sigma}_{31}^{*2}+2F\hat{\sigma}_{12}^{*2}\}^{1/2}\\ =&\{(A+B+4C-2E)\ tr^2(\boldsymbol{a}_1\boldsymbol{s}^*)+(A+4B+C-2D)\ tr^2(\boldsymbol{a}_2\boldsymbol{s}^*)\\ &+2(-A+2B+2C-D-E+F)\ tr(\boldsymbol{a}_1\boldsymbol{s}^*)\ tr(\boldsymbol{a}_2\boldsymbol{s}^*)\\ &+2(F-D)\ tr(\boldsymbol{a}_1\boldsymbol{s}^{*2})+2(F-E)\ tr(\boldsymbol{a}_2\boldsymbol{s}^{*2})+(D+E-F)\ tr\ \boldsymbol{s}^{*2}\}^{1/2}\equiv\delta\end{aligned}\tag{4}$$

where $\boldsymbol{a}_i=\boldsymbol{n}_i\otimes\boldsymbol{n}_i$, $i=1, 2, 3$ (not summation), A to F are the material parameters, and δ is the size of dynamic yield surface. For the case of $\boldsymbol{\alpha}=\boldsymbol{0}$, Eq. (4) produces the orthotropic hardening model of Hill (1950), while for $A=B=C=1$ and $D=E=F=3$, this reduces to von Mises' type kinematic hardening with $J=\{tr(s\text{-}\alpha)^2\}^{1/2}$ for an isotropic material.

The corotaional rate of the back stress α is assumed to be

$$\overset{c}{\alpha}=\dot{\alpha}-\omega_k\alpha+\alpha\omega_k=\frac{2}{3}h_a\ \boldsymbol{D}^p-c_r(\dot{\bar{\varepsilon}}^p)^s\alpha-c_s\alpha\tag{5a}$$

$$\omega_k=\boldsymbol{W}-\boldsymbol{W}_k^p\tag{5b}$$

$$\boldsymbol{W}_k^p\equiv\boldsymbol{\Phi}\boldsymbol{\Omega}_k^p=\frac{1}{2}\boldsymbol{\Phi}\rho\left(\alpha\frac{\partial J}{\partial\sigma}-\frac{\partial J}{\partial\sigma}\alpha\right)=\frac{1}{2}\rho(\alpha\boldsymbol{D}^p-\boldsymbol{D}^p\alpha)\tag{5c}$$

where h_a, c_r, c_s, s, and ρ are the material constants, and $\boldsymbol{W}_k^p$ and ω_k are the plastic spin and its associated constitutive spin for the back stress, respectively. The $\boldsymbol{\Phi}\equiv[(J-\sqrt{2}k)/V]^{1/n}$ is the overstress function of the state variables. The last term of Eq. (5c) can be derived from the definition of $\boldsymbol{D}^p=\boldsymbol{\Phi}(\partial J/\partial\sigma)$. The $\dot{\bar{\varepsilon}}^p\equiv(2/3\ \boldsymbol{D}^p\!:\!\boldsymbol{D}^p)^{1/2}$ is the rate of the equivalent plastic strain.

Since the corotational rate of the orthotropic axes with respect to the constitutive spin ω_o should be zero as:

$$\overset{c}{\boldsymbol{n}}_i=\dot{\boldsymbol{n}}_i-\omega_o\boldsymbol{n}=\boldsymbol{0}\tag{6}$$

the orthotropic axes can be obtained with the following proposition for ω_o (Dafalias 1993):

$$\omega_o=\boldsymbol{W}-\boldsymbol{W}_o^p=x\boldsymbol{\Omega}^E+(1-x)(\boldsymbol{W}-\boldsymbol{W}_o^{p*})\tag{7a}$$

$$x=\exp(-c\bar{\varepsilon}^p)\tag{7b}$$

where $\boldsymbol{\Omega}^E$ is the Eulerian spin, $\bar{\varepsilon}^p$ is a scalar measure of equivalent plastic strain, and x is the material parameter describing the level of material's transition to the plastic spin $\boldsymbol{W}_o^{p*}$ at its full orthotropy via the parameter c. Since $x=1$ at $\bar{\varepsilon}^p=0$ and $x=0$ at $\bar{\varepsilon}^p=\infty$, it is seen from Eq. (7a) that the constitutive spin of orthotropic hardening vary from the initial Eulerian spin $\boldsymbol{\Omega}^E$ to the final $\boldsymbol{W}-\boldsymbol{W}_o^{p*}$.

3. Application to simple shear

The combined hardening model is applied to the case of simple shear, which can describe the deformation of a solid cylinder face element during the fixed-end torsion tests. Therefore, the equations of simple shear are now summarized in this section for a subsequent discussion on the effect of constitutive spins within the combined hardening model. The velocity gradient components for simple shear strain $\gamma(t)$ in x_1-x_2 plane, are given by

$$\begin{aligned} &D_{12}=D_{21}=W_{12}=-W_{21}=\dot{\gamma}/2 \\ &D_{ij}=W_{ij}=0 \qquad \text{for other } i,\ j \text{ combinations} \end{aligned} \tag{8}$$

where x_i, $i=1$, 2, 3, are the Cartesian coordinates of current position of a material point. Since this work is concerned with large plastic deformations with negligible small elastic strains, a rigid-plastic material response will be for simplicity assumed, hence, $\boldsymbol{D}^p=\boldsymbol{D}$.

For the particular case of cubically orthotropic symmetries where $A=B=C=a$ and $D=E=F=b$, the projection of the intersection of the three dimensional yield surface Eq. (4) with the plane of $\sigma^*_{11}+\sigma^*_{22}=0$ onto the $\sigma^*_{11}-\sigma^*_{12}$ plane reduces to

$$\begin{aligned} J^2&=[2b+(6a-2b)\cos^2 2\phi]\ \sigma^{*2}_{11}+[2b+(6a-2b)\sin^2 2\phi]\ \sigma^{*2}_{12} \\ &\quad+(6a-2b)\sin 4\phi\ \sigma^*_{11}\ \sigma^*_{12} \\ &=(6a-2b)[tr^2(\boldsymbol{a}_1\boldsymbol{s}^*)+tr^2(\boldsymbol{a}_2\boldsymbol{s}^*)+tr(\boldsymbol{a}_1\boldsymbol{s}^*)\ tr(\boldsymbol{a}_1\boldsymbol{s}^*)]+b\ tr\ \boldsymbol{s}^{*2}=\delta^2 \end{aligned} \tag{9}$$

$$-\sigma^*_{11}=\sigma^*_{22}=\delta\ \mathrm{sgn}(\dot{\gamma}\ \cos 2\phi)\ \left(\frac{3a}{b}-1\right)\ \sin 2\phi\ \left[6a\left(\frac{3a}{b}+\tan^2 2\phi\right)\right]^{-1/2} \tag{10a}$$

$$\sigma^*_{12}=\delta\ \mathrm{sgn}(\dot{\gamma})\ \left[\frac{1}{6a}\ \left(1+\left(\frac{3a}{b}-1\right)\ \cos^2 2\phi\right)\right]^{1/2} \tag{10b}$$

$$\delta=\sqrt{2}k+V\left[\frac{2}{3}tr\left(\frac{\partial J}{\partial \sigma}\right)^2\right]^{-1/2n}(\dot{\varepsilon})^{1/n}=\sqrt{2}k+V^*(\dot{\varepsilon})^{1/n} \tag{10c}$$

$$\mathrm{sgn}(*)=\text{sign of } * \tag{10d}$$

where ϕ is the counterclockwise angle from x_1-axis to the orthotropic axis $\boldsymbol{n}_1$, with following differential equations for the back stress $\boldsymbol{\alpha}$:

$$\frac{d\alpha_{11}}{d\gamma}=-\frac{d\alpha_{22}}{d\gamma}=-\mathrm{sgn}(\dot{\gamma})\frac{c_k}{\sqrt{3}}\ \alpha_{11}+(1-\rho\alpha_{11})\ \alpha_{12} \tag{11a}$$

$$\frac{d\alpha_{12}}{d\gamma}=-\mathrm{sgn}(\dot{\gamma})\frac{c_k}{\sqrt{3}}\alpha_{12}-(1-\rho\alpha_{11})\ \alpha_{11}+\frac{1}{3}h_a \tag{11b}$$

$$c_k=c_r(\dot{\varepsilon})^{s-1}+\frac{c_s}{\dot{\varepsilon}}=c_r\left(\frac{|\dot{\gamma}|}{\sqrt{3}}\right)^{s-1}+\frac{\sqrt{3}\ c_s}{|\dot{\gamma}|}. \tag{11c}$$

And, the variations of a and b, which are in charge of the distortional hardening of yield surface, are assumed as:

$$a=(1-a_s)\ \exp(-c_a|\gamma|)+a_s \tag{12a}$$

$$b=(3-b_s)\ \exp(-c_b|\gamma|)+b_s \tag{12b}$$

where a_s and b_s are the saturated values of a and b with increasing plastic deformations, and c_a and c_b are the material constants.

The angle ϕ of the orthotropic axis can be obtained from Eqs. (6) and (7), which yield the following differential equation:

$$\frac{d\phi}{d\gamma}=\frac{1}{2}\left[(1-x)(\eta\ \cos2\phi-1)-x\frac{2}{\gamma^2+4}\right] \tag{13a}$$

$$x=\exp(-c|\gamma|) \tag{13b}$$

where η is the material parameter implying the level of full orthotropy, and c is the scalar-valued transition coefficient. It is noted from Eq. (13a) that, at $\gamma=0$, $x=1$ and $d\phi/d\gamma=-1/4$, while at $\gamma=\infty$, $x=0$ and $d\phi/d\gamma=(\eta\cos2\phi-1)/2$, therefore, the saturated value of ϕ, the $\phi_e=[\cos^{-1}(1/\eta)]/2$.

4. The effect of constitutive spins

Within the framework of the combined isotropic/kinematic/distortional/orientational hardening model at large plastic deformations (Cho and Dafalias 1996), complex experimental phenomena of Montheillet, *et al.* (1984), in particular, oscillatory axial stresses of fixed-end torsion tests for *α-Fe*, *Al* and *Cu* with plastic shear deformations, were successfully, at least qualitatively, simulated for different strain rates. Since this hardening model is a combination of classical isotropic/kinematic and orthotropic hardening models, it can therefore portray physically different features of residual stresses and texture developments caused by finite plastic deformations within one constitutive formulation. In addition to the novel concept of the combination of hardenings, the introduction of multiple constitutive spins is of cardinal importance, i.e., the back stress and orthotropy have their own associated spins. It is noted that, since Montheillet, *et al.* (1984) did not provide any experimental shear stress data of their fixed-end torsion tests except for *α-Fe* at the strain rate of 0.5, some educational guesses were needed especially for *Al* and *Cu* in the process of simulation.

Since the investigation of the effects of these multiple constitutive spins on finite plastic simulations is the focus of this section, some calibrated material parameters of Cho and Dafalias (1996) will be again used (interested readers may be recommended to refer for more detail to their work) and a few observations about the characteristics of the analytical equations for simple shear are pertinent. In simple shear, Eqs. (11) of kinematic hardening part yield negative α_{22}, while Eqs. (10) of orthotropic hardening part can produce positive σ^*_{22}. More comprehensive study for kinematic hardening (Dafalias 1990) reveals that α_{22} with reasonable values for the material parameters converges in a smooth fashion within compressive region. Then, the complex phenomena of axial stress variations from negative to positive and/or oscillatory negative can be obtained by the capacity of orthotropic hardening, i.e., the distortional hardening via the variations of parameters a and b, as well as the orientational hardening via the variations of orthotropic angle ϕ (Dafalias and Rashid 1989), which are closely related to the variations of the plastic spins. Fig. 1 shows the representative simulations in Cho and Dafalias (1996) for three materials of *α-Fe*, *Al* and *Cu* at the equivalent strain rate of 0.5. Four simulation curves of axial stresses of the three materials and the shear stress of *α-Fe* only are given. For the axial stress $-\sigma_{22}$ of *α-Fe* and *Cu*, initial positive stress (i.e., σ_{22} is in fact negative) becomes negative as shear strain increases. Reminding that $\boldsymbol{\sigma}=\boldsymbol{\alpha}+\boldsymbol{\sigma}^*$ and α_{22} is negative in simple shear, it is clear that α_{22} of kinematic hardening initially governs while later positive σ^*_{22} of orthotropic hardening becomes predominant. On the other hand, the axial stress σ_{22} of *Al* remains throughout in compressive region with monotonically increasing shear strain. Therefore, one may guess that the oscillatory σ_{22} can be obtained by the addition of predominant negative α_{22} and oscillatory

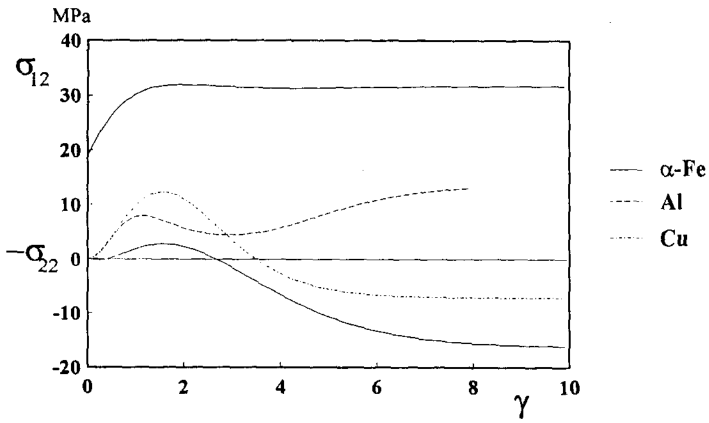

Fig. 1 Simulation of experimental results for *α-Fe, Al* and *Cu* at the equivalent strain rate of 0.5 (after Cho and Dafalias 1996).

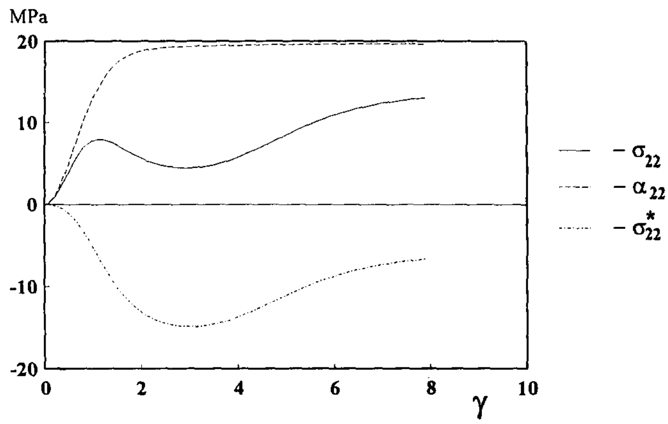

Fig. 2 The variations of α_{22}, σ^*_{22} and σ_{22} for *Al*.

positive σ^*_{22}, which are shown in Fig. 2 describing the combination of the axial stresses for *Al* at the equivalent strain rate of 0.5 and 200℃. More investigations for the material parameters in charge of the oscillatory positive axial stress σ^*_{22} will be followed subsequently.

In the formulation of the combined hardening model there are two constitutive spins of ω_k and ω_o for the back stress and orthotropic axes, respectively. Since each constitutive spin has its corresponding angle to which the associated director-vector frame is referred, it is worthwhile to investigate the variations of the angles, denoted henceforth by ϕ_k and ϕ_o, for the former and latter, respectively. From the differential equation of $d\phi_k/d\gamma=(W_{12}^{pk}/W_{12}-1)/2=(\rho\alpha_{11}-1)/2$, the variable angle ϕ_k with shear deformations is given in Fig. 3(a), where the vertical axis does not represent the real value of ϕ_k, but it just shows the trend of the variations of ϕ_k. To have the real ϕ_k, the value of Fig. 3(a) should be added to the initial value of ϕ_k at $\gamma=0$. For *Al* and *Cu*, the continuous decrease of ϕ_k with increasing shear strain occurs due to very low values of ρ (even zero for *Cu*). It is noted that $\rho=0$ means no plastic spin terms in kinematic hardening, then $W_{12}=\omega_{k,12}=-\dot{\phi}_k=\dot{\gamma}/2>0$, i.e., ϕ_k is continuously decreasing. However, for *Al* having a relatively high positive value of ρ, the ϕ_k is seen to converge to a saturated value with increasing

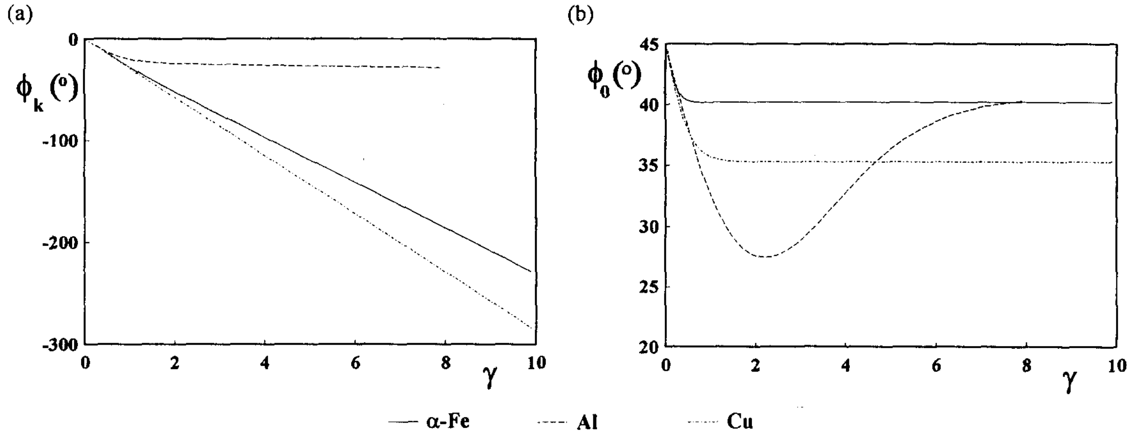

Fig. 3 The variations of the angles: (a) ϕ_k and (b) ϕ_o for *α-Fe, Al* and *Cu.*

Table 1 Model constants for *α-Fe* at 800℃, *Al* at 200℃, and *Cu* at 300℃ (after Cho and Dafalias 1996)

Constants	*α-Fe*	*Al*	*Cu*
ρ (MPa^{-1})	0.01634	0.05	0
η	6	7.2	3
c	5	0.03	3

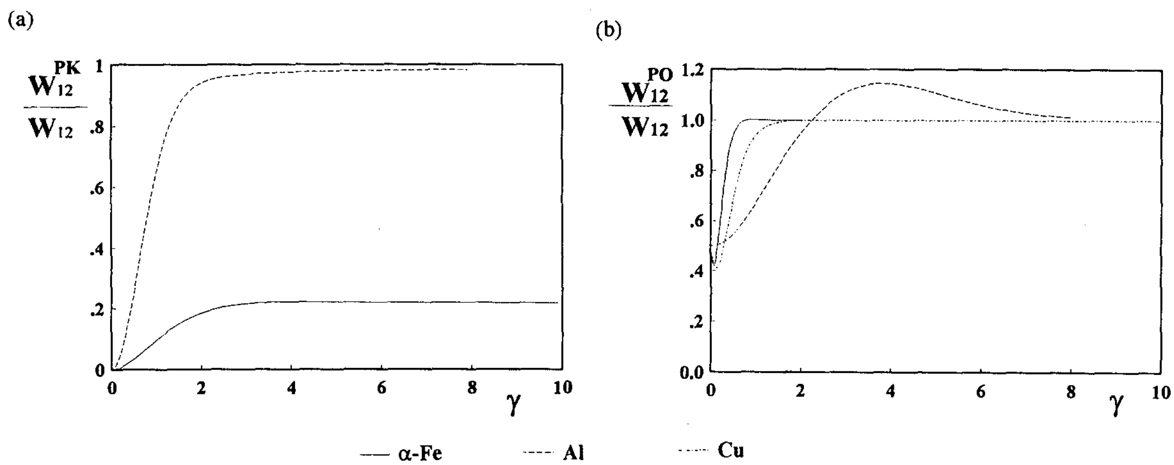

Fig. 4 The ratios of (a) W_{12}^{pk}/W_{12} and (b) W_{12}^{po}/W_{12} for *α-Fe, Al* and *Cu.*

deformations. In Fig. 3(b), the variations of ϕ_o with increasing shear strains are shown using the values of Table 1 for *α-Fe, Al* and *Cu* (Cho and Dafalias 1996). As discussed in the previous section, the η decides the saturated ϕ_o while the c controls the speed of transition of the constitutive spin from $\boldsymbol{\Omega}^E$ to $\boldsymbol{W}-\boldsymbol{W}_o^{p*}$. Novel feature of oscillation particularly for Al can be explained by $\eta=7.2$ and $c=0.03$, which makes the ϕ_o decreasing due to the big influence of the Eulerian spin at the beginning and later increasing back to the saturated value of ϕ_o of 41 degrees. Notice that the variations of ϕ_o for *Al* is very close to the trend of σ^*_{22} in Fig. 2. However, for *α-Fe* and *Cu* fast changes of the constitutive spin due to large values of the parameter c help the ϕ_o to converge smoothly to its saturated value.

Using Table 1 again, Fig. 4(a) shows the variations of W_{12}^{pk}/W_{12} with increasing shear strains for *α-Fe, Al* and *Cu*. Since $W_{12}^{pk}/W_{12}=\rho\alpha_{11}$, small ratios for *α-Fe* and *Cu* are seen due to the small values of ρ's. For *Al* with a relatively high value of ρ, the ratio rapidly becomes close to 1, i.e., $\omega_{k,12}\cong 0$, with shear deformations. Similarly, Fig. 4(b) gives the variations of W_{12}^{po}/W_{12} for *α-Fe, Al* and *Cu*. Since $W_{12}^{po}/W_{12}=2\ d\phi_o/d\gamma+1$ in simple shear, Eq. (13a) yields

$$\frac{W_{12}^{po}}{W_{12}}=(1-x)\ \eta\ \cos 2\phi_o+x\,\frac{\gamma^2+2}{\gamma^2+4}. \tag{14}$$

Notice that $x=1$ at $\gamma=0$ and $x=0$ at $\gamma=\infty$. The W_{12}^{po}/W_{12} of *α-Fe* and *Cu* with big values of η and c initially decreases for a short period and later increases fast up to 1 at $\gamma=\infty$. However, for *Al* with a small c, the second term of the right-hand side in Eq. (14) governs in the beginning. As the x becomes smaller with increasing deformation, the influence of the first term grows followed by an oscillation of the ratio, which seems to show same trend as the oscillatory transition of the angle ϕ_o, in Fig. 3(b). Based on these observations, it is seen that this orientational hardening (the variations of the angle ϕ_o) can capture oscillatory responses of axial stress in simple shear via the parameters η and c.

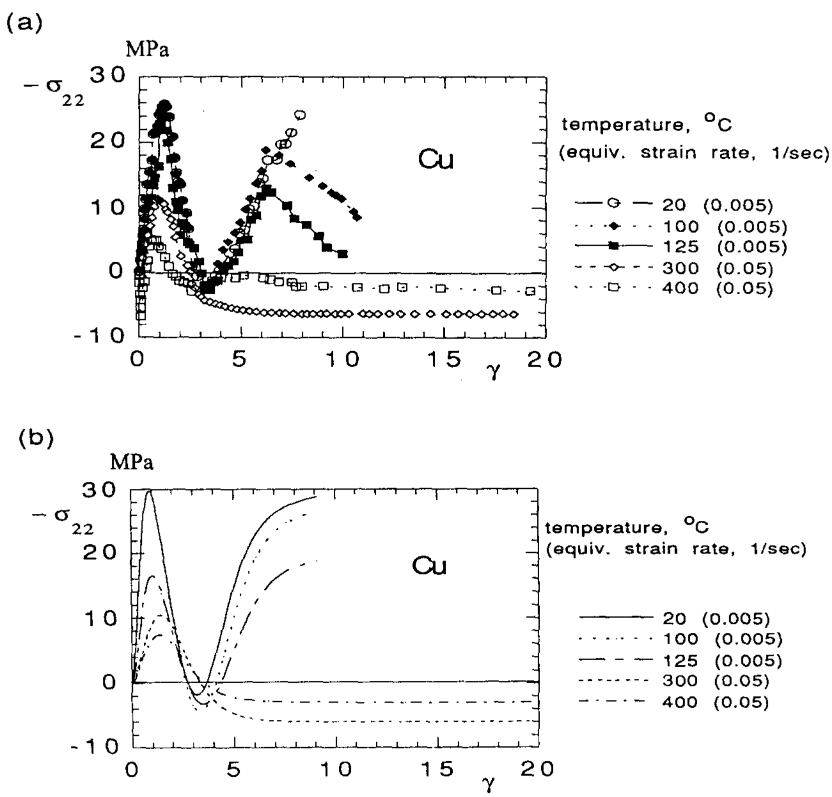

Fig. 5 (a) Experimental and (b) simulational axial stress/strain dependence on temperature for *Cu*.

Table 2 Model constants for the simulations shown in Figs. 5 and 6 for *Cu*

Constants	20℃	100℃	125℃	300℃	400℃
δ (MPa)	170	170	120	99	50
h_a (MPa)	1100	1100	500	245	180
ρ (MPa^{-1})	0.018	0.018	0.02	0	0
c_k	1.5	1.5	1.8	2.5	2.7
a_s	0.5	0.5	0.5	0.5	0.5
b_s	0.5	0.5	0.5	0.5	0.5
c_a	1	1	1	1	1
c_b	1	1	1	1	1
η	10	9	8	3	2
c	0.03	0.03	0.03	3	3

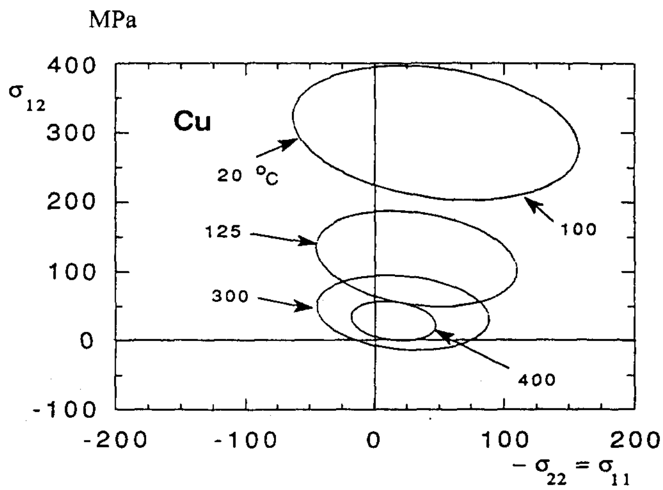

Fig. 6 Dependence of yield surface on temperature for *Cu* at $\gamma = 1.5$.

In the present paper, temperature effect on the response of simple shear is another important aspect to be discussed. Similar to the simulations of *Al* at various temperatures in Cho and Dafalias (1996), Fig. 5(a) shows axial stress variations for *Cu* with shear deformations at different temperatures from the aforementioned experiments, and their simulations are given in Fig. 5(b) using the material constants in Table 2. It is seen that two results are in a good agreement. Fig. 6 shows the dependence of the yield surface on temperature with the corresponding yield surfaces at $\gamma = 1.5$ for the cases of different temperatures. This gives reasonable interpretation that, as the temperature increases, the center of the yield surface, representing the back stress, becomes smaller and the size of yield surface is reduced.

As for the ratio of plastic spin to total spin, Figs. 7 show its variation with shear deformation, with the material constants in Table 3 for *Al* at different temperatures, for which the simulations and their associated yield surfaces were discussed in Cho and Dafalias (1996). With the rise of temperature, the converging value of W_{12}^{pk}/W_{12} simply becomes smaller as in Fig. 7(a) while oscillatory trend of $W_{12}^{p\alpha}/W_{12}$ with shear deformation tends to be slower and smaller as in Fig.

Table 3 Model constants for *Al* (after Cho and Dafalias 1996)

Constants	20℃	100℃	200℃	300℃	350℃
η	15	12	7.2	6	5
c	0.03	0.03	0.03	0.03	0.03

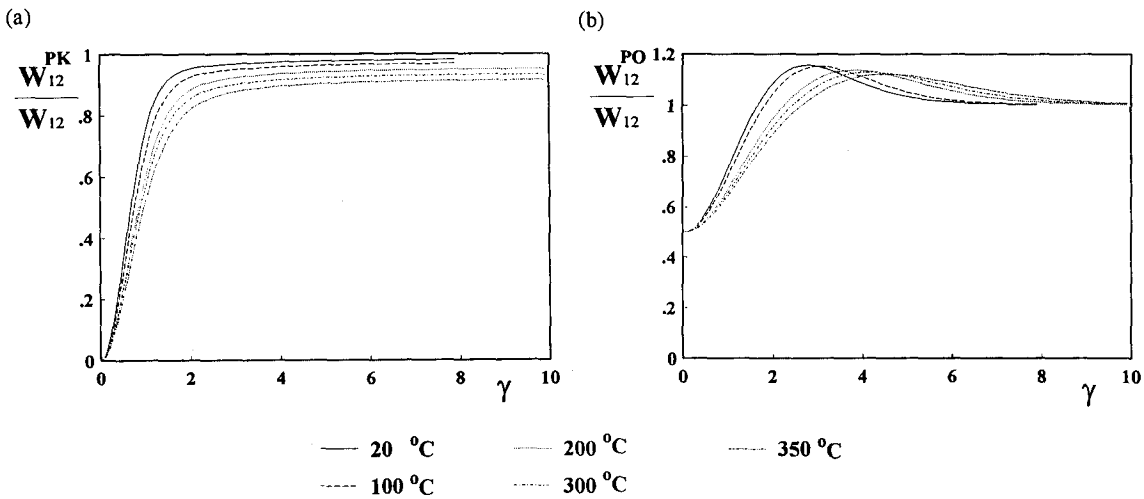

Fig. 7 The variations of (a) W_{12}^{pk}/W_{12} and (b) W_{12}^{po}/W_{12} with temperature for *Al*.

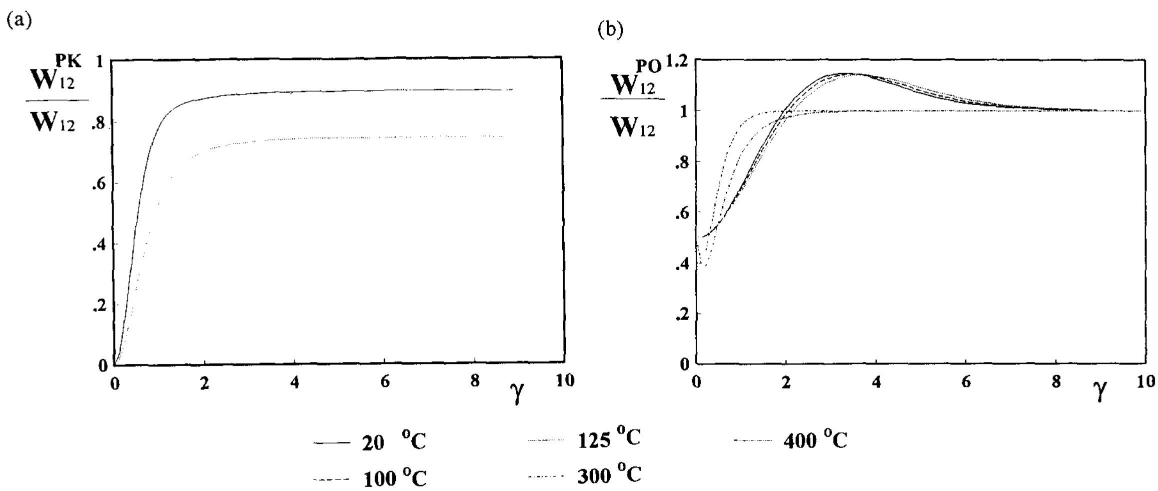

Fig. 8 The variations of (a) W_{12}^{pk}/W_{12} and (b) W_{12}^{po}/W_{12} with temperature for *Cu*.

7(b). Fig. 8(a) gives for *Cu* similar trend of W_{12}^{pk}/W_{12} decreasing with the increase of temperature. It is noted that the ratios for 20℃ and 100℃ are overlapped, and those for 300℃ and 400℃ are zeros since $\rho=0$. The variation of W_{12}^{po}/W_{12} for *Cu* in Fig. 8(b) has the same trend, as in Fig. 7(b) for *Al*, for the temperatures of 20℃, 100℃ and 125℃. While at high temperatures such as 300℃ and 400℃, the transition trend is altered to that of *α-Fe* and *Cu* in Fig. 4(b), without having a big oscillation around $\gamma=3.5$, i.e., the material properties are considerably changed so that initial osillatory compressive axial stress becomes tensile stress with increasing shear deformations.

5. Conclusions

Simple shear analyses were successfully performed within a combined anisotropic hardening model in order to simulate the fixed-end torsion experiments. Two representative variations of axial stresses from compressive (negative) to tensile (positive) or oscillatory compressive could be explained by the orthotropic hardening part, capturing tensile axial stresses either smooth or oscillatory, in addition to compressive axial stresses of kinematic hardening. The oscillatory trend of tensile axial stresses was shown to be in inseparable relation to the variations of the plastic spins in the elastoplastic constitutive formulation, especially via the saturated values and the pace thereto of the angles of orthotropic axes. On the other hand, the variations of the material parameters a and b with increasing shear deformations control the size as well as the distortion of yield surface. As the temperature increases, the size of yield surface reduces and the relatively long influence, at the beginning, of the Eulerian spin in charge of oscillatory axial stresses at low temperature becomes less with even non-oscillatory responses due to the fast change to full orthotropy.

References

Cho, H.W. and Dafalias, Y.F. (1996), "Distortional and orientational hardening at large viscoplastic deformations," *Int. J. Plasticity,* **12**(7), 903-925.

Dafalias, Y.F. (1985), "The plastic spin," *ASME J. Applied Mechanics,* **52**, 865-871.

Dafalias, Y.F. (1990), "The plastic spin in viscoplasticity," *Int. J. Solids Structures,* **26**, 149.

Dafalias, Y.F. (1993), "On multiple spins and texture development. Case study: kinematic and orthotropic hardening," *Acta Mechanica,* **100**, 171-194.

Dafalias, Y.F. and Cho, H.W. (1989), "Verification of the spin concept in viscoplasticity", *Advances in Plasticity* 1989 (Khan, A.S. and Tokuda, M. eds.), 287-290, 2nd Int. Symp. on Plasticity and its Current Applications, Mie, Japan, 1989. New York: Pergamon 1989.

Dafalias, Y.F. and Rashid, M.M. (1989), "The effect of plastic spin on anisotropic material behavior," *Int. J. Plasticity,* **5**, 227-246.

Hill, R. (1950), *The Mathematical Theory of Plasticity*, Oxford University Press, London.

Montheillet, F., Cohen, M, and Jonas, J.J. (1984), "Axial stresses and texture development during the torsion testing of Al, Cu and α-Fe," *ACTA Metallurgica,* **32**(11), 2077-2089.